

Field monitoring of wind effects on a super-tall building during typhoons

Lunhai Zhi¹, Q.S. Li^{*2}, J.R. Wu^{2,3} and Z.N. Li¹

¹Key Laboratory of Building Safety and Energy Efficiency of Ministry of Education,
College of Civil Engineering, Hunan University, Changsha, Hunan, P.R. China

²Department of Building and Construction, City University of Hong Kong,
Tat Chee Avenue, Kowloon, Hong Kong

³School of Civil Engineering, Guangzhou University, Guangzhou, Guangdong, P.R. China

(Received March 4, 2010, Accepted December 15, 2010)

Abstract. This paper presents the field measurement results of wind effects on a super-tall building (CITIC Plaza, 391 m high) located in Guangzhou. The field data such as wind speed, wind direction and acceleration responses were simultaneously and continuously recorded from the tall building by a wind and vibration monitoring system during two typhoons. The typhoon-generated wind characteristics including turbulence intensity, gust factor, peak factor, turbulence integral length scale and power spectral density of fluctuating wind speed were presented and discussed. The dynamic characteristics of the tall building were determined based on the field measurements and compared with those calculated from a 3D finite element model of the building. The measured natural frequencies of the two fundamental sway modes of the building were found to be larger than those calculated. The damping ratios of the building were evaluated by the random decrement technique, which demonstrated amplitude-dependent characteristics. The field measured acceleration responses were compared with wind tunnel test results, which were found to be consistent with the model test data. Finally, the serviceability performance of the super-tall building was assessed based on the field measurement results.

Keywords: wind effect; reinforced concrete structure; tall building; typhoon; full-scale measurement; dynamic response; wind tunnel test.

1. Introduction

Field measurements of wind effects on structures are very useful, particularly for calibrating codes of practice for wind-resistant design of structures and for incorporation into useable wind tunnel simulations and CFD numerical modeling as well as structural analysis. In fact, it has been recognized that field measurement is the most reliable tool for investigation of wind characteristics in atmospheric boundary layer and evaluation of wind effects on buildings and structures.

With the development of measurement devices and data acquisition techniques during the last three decades, extensive field measurement studies on wind effects on tall buildings have been

* Corresponding Author, Dr., E-mail: bcqqli@cityu.edu.hk

carried out (Ohkuma *et al.* 1991, Littler and Ellis 1992, Li *et al.* 1998, 2004a, 2004b, 2005, 2006, Jeary 1986, Kijewski-Correa 2003, Tamura and Suganuma 1996, Campbell *et al.* 2007, Pirnia *et al.* 2007), including the measurement programs on four Chicago tall buildings currently being undertaken by Notre Dame University and the University of Western Ontario (Kijewski-Correa 2003) and on ten super-tall buildings in Hong Kong and Mainland China by City University of Hong Kong (Li *et al.* 1998, 2004a, 2004b, 2005, 2006). Significant efforts have been made to investigate wind speed and turbulence characteristics above city central districts based on filed measurements. The dynamic behaviors such as natural frequencies, mode shapes and damping ratios of the tall buildings were identified and the wind-induced vibrations of these high-rise structures were investigated. However, as commented by Tamura *et al.* (2005), the chance to conduct full-scale measurements is very limited, and obtained data are very important and valuable. In particular, literature review reveals that comprehensive full-scale measurements of wind effects on super-tall buildings (building height > 350 m) have rarely been conducted during typhoons in the past. There is therefore a strong case for carrying out such a study, since a number of super-tall buildings are being designed and constructed throughout the world.

CITIC Plaza, 391m high with 80 floors, located in the central district of Guangzhou, is the world's tallest building fully made of reinforced concrete. Guangzhou is located at an active typhoon generating area. This super-tall building may be subjected to severe wind forces induced by typhoons. All these facts made it necessary to investigate the performance of the super-tall building under typhoon conditions. A wind and structural monitoring system was thus installed on CITIC Plaza by the authors in 2005 and it has been operating since then. The main goal of the monitoring study is for further understanding typhoon-generated wind characteristics above a typical urban area and investigating the performance of the super-tall building under strong winds.

This paper briefly introduces the monitoring system and then presents selected field measured results such as wind speed, wind direction and acceleration response which were simultaneously and continuously recorded by the monitoring system from the tall building during the passage of Typhoon Damrey on September 24, 2005 and Typhoon Pabuk on August 10, 2007. Detailed analysis of the field data was carried out to investigate the wind effects on the super-tall building. The characteristics of the typhoon-generated wind, the dynamic characteristics and responses of the tall building were determined based on the field measurements. Moreover, the serviceability of the super-tall building was assessed based on the data recorded during the typhoons. In fact, monitoring the performance of the super-tall building under typhoon conditions can provide useful validation of design procedures and assurance of acceptable behaviour. Therefore, the field measurements of wind effects on the tall building are very useful in gaining an understanding of the wind-resistant design and the habitability of super-tall buildings.

2. Description of the structure and monitoring system

CITIC Plaza with an 80-storey superstructure (shown in Fig. 1(a)) and 331 m high above ground level is a commercial tall building. Two antennas with height of 60 m were built atop the eastern and western wings of the building. The total height of the building is thus 391 m. CITIC Plaza is located in the central district of Guangzhou, Guangdong province, China, and is surrounded by a number of buildings including some tall buildings with a height of more than 100 m (shown in Fig. 1(b)). The site around the building can be regarded as terrain *C* (an urban area) according to the Chinese



Fig. 1(a) Elevation view of CITIC Plaza



Fig. 1(b) Photographic views to the east of CITIC Plaza

National Load Code (GB50009-2001). CITIC Plaza is a tube-in-tube reinforced concrete structure with three outrigger belts located at the 25th, 44th and 65th floors to stiffen the lateral stiffness of the building. The basic platform of the building is square with 46.8 m in each side. The building is slender with a height to width ratio (aspect ratio) of 6.9. Hence, it is a wind sensitive structure.

The basic make-up of the monitoring system developed by the authors includes two major parts: a data acquisition unit (DAU) and two groups of sensors including anemometers and accelerometers. Two anemometers (a R.M. Young's propeller anemometer (Model 05106) and a 3-D ultrasonic anemometer) were installed at height of 352.5 m on the mast built above the eastern wing of the building to record the wind speed and wind direction over a typical urban area. In order to measure the dynamic responses of the tall building under dynamic excitations such as wind and earthquake, two accelerometers were placed orthogonally along the two main axes (directions 1 and 2 shown in Fig. 2(a) on the 76th floor. Photos of two anemometers of the monitoring system are shown in Fig. 2(b) and (c), while data acquisition instrument is shown in Fig. 2(d). The system can monitor wind speed, wind direction and the structural acceleration responses of the super-tall building in real-time manner and provide information and data for evaluating the safety and serviceability conditions of



Fig. 2(a) Top view of CITIC Plaza



Fig. 2(b) Propeller anemometer



Fig. 2(c) Ultrasonic anemometer



Fig. 2(d) Data acquisition instrument

Table 1 Typhoon information on the field measurement results presented in this paper

| Typhoons | Date | Wind direction | Wind speed record length (minutes) | Peak gust (m/s) |
|----------|-------------------------------|----------------|------------------------------------|-----------------|
| "Damrey" | 24th September, 2005 | NE | 3200 | 29.4 |
| "Pabuk" | 10 th August, 2007 | NE | 550 | 22 |

the super-tall building under wind actions or earthquake excitations. For the data analyzed and presented in this paper, the wind speed, wind direction and wind-induced acceleration response were simultaneously sampled and digitized at 10 Hz by the monitoring system during the passages of Typhoons Damrey and Pabuk. Table 1 presents the relevant information on the typhoons.

3. Wind characteristics

3.1 Mean wind speed and direction

Figs. 3(a) and (b) show the horizontal mean wind speed and wind direction, which were measured

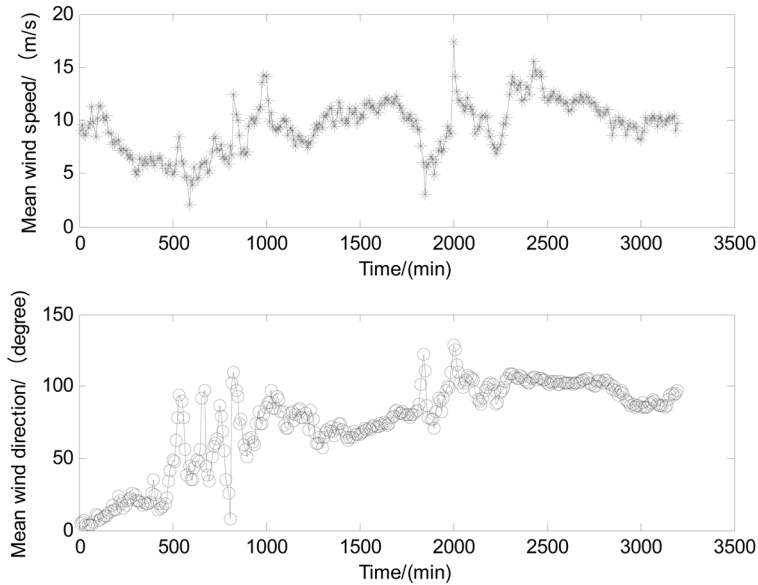


Fig. 3(a) 10 min mean wind speed and direction during Typhoon Damrey

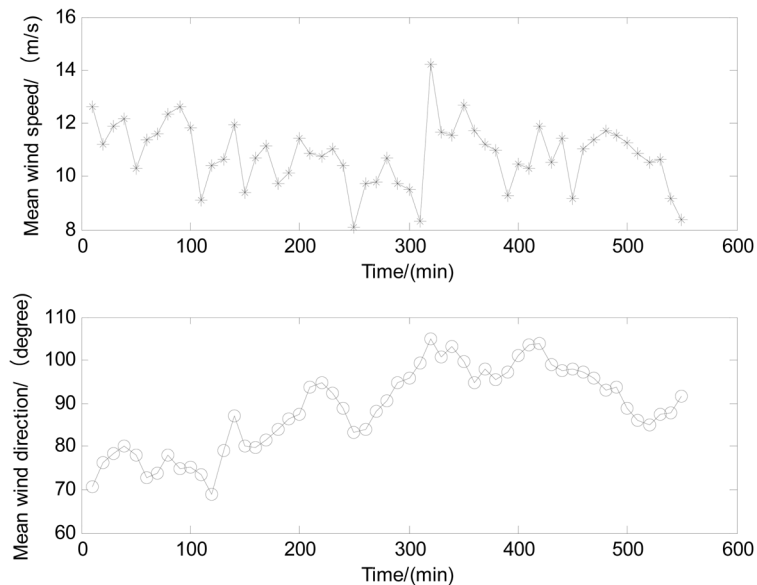


Fig. 3(b) 10 min mean wind speed and direction during Typhoon Pabuk

from the ultrasonic anemometer during the typhoons. The maximum instantaneous wind speeds measured atop CITIC Plaza during Typhoons Damrey and Pabuk were 29.4 and 22 m/s, respectively. The maximal 10-min mean wind speed recorded during the passages of Typhoons Damrey and Pabuk were 17.3 m/s and 14.3 m/s, respectively. The 10-min mean wind direction during Typhoons Damrey and Pabuk varied in ranges of 3° ~ 129° and 69° ~ 105° with the mean wind direction of 74° and 89° , respectively. The records illustrate the mean wind direction during Typhoon Pabuk was

relatively stable, while the variation of wind direction was larger during the passage of Typhoon Damrey.

3.2 Turbulence intensity

Turbulence intensity is an important parameter for describing the turbulence characteristics of wind flows. It can be obtained by the following equation

$$I_i = \sigma_i / U, (i = u, v, w) \quad (1)$$

where U is 10 min mean wind speed; σ_i is standard deviation of fluctuating wind speed component; u , v and w denote the longitudinal, lateral and vertical components of wind speed.

Fig. 4 shows the polar plots of longitudinal, lateral and vertical turbulence intensities, respectively, of 10 min duration during the typhoons. It is found that the values of turbulence intensities for the sectors 0-30, 30-60, 60-90 and 90-120 degrees are similar. It appears that the turbulence intensities at such a high level over an urban area are not sensitive to the terrain conditions around the building. The average values of the turbulence intensity in the longitudinal, lateral and vertical directions were 0.14, 0.12 and 0.10, respectively. The ratio of the turbulence intensities among the three components is $I_u : I_v : I_w = 1 : 0.86 : 0.71$, which is different from the statistical result $I_u : I_v : I_w = 1 : 0.75 : 0.50$ obtained in the near-neutral atmospheric conditions by Solari and Piccardo (2001). This can be attributed to the differences in the heights where the turbulence intensities were measured. In the guidelines recommended by the Architectural Institute of Japan (AIJ-RLB-1996), the longitudinal turbulence intensity can be estimated by the empirical expression: $I_u = 0.1(z/Z_G)^{-\alpha-0.5}$. As the height of the anemometer location is 352.5 m above ground level, the longitudinal turbulence intensity calculated from this equation is 0.13. The measured mean value is actually in good agreement with the predicted one, implying that the empirical formula recommended by AIJ is applicable to engineering practice. Fig. 5 shows the variations of turbulence intensities measured

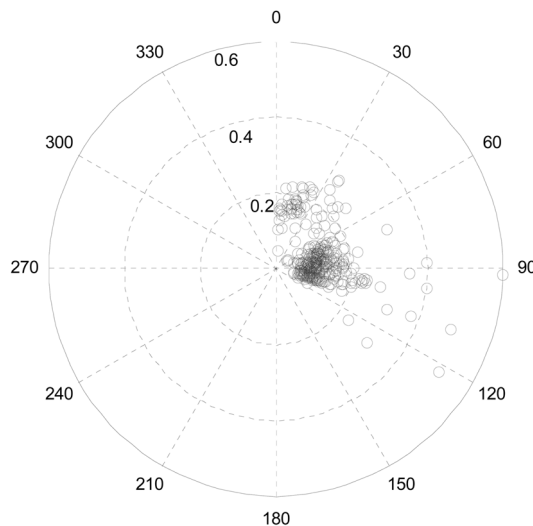


Fig. 4(a) Variation of the longitudinal turbulence intensity with the mean wind direction

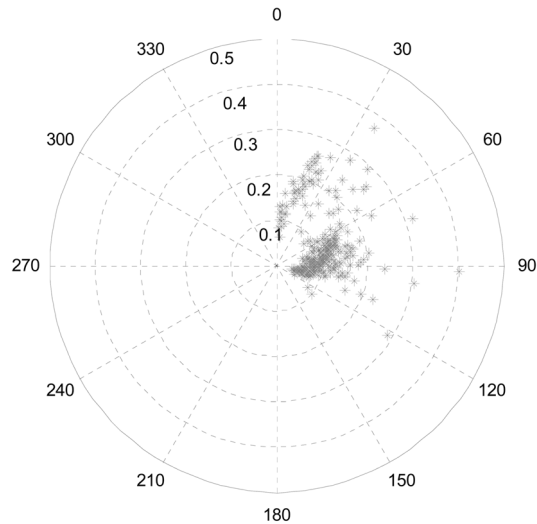


Fig. 4(b) Variation of the lateral turbulence intensity with the mean wind direction

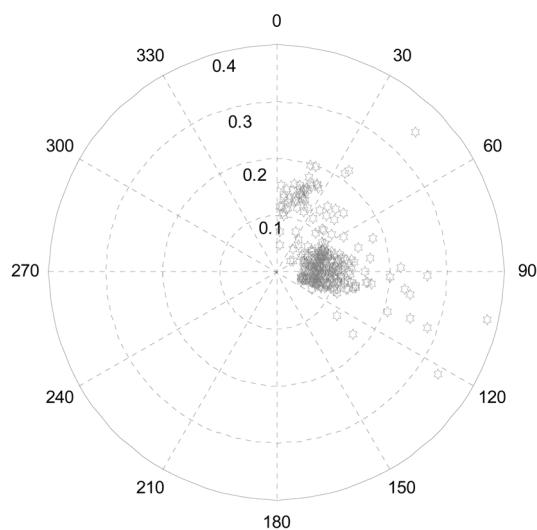


Fig. 4(c) Variation of the vertical turbulence intensity with the mean wind direction

by the ultrasonic anemometer with the mean wind speed. It can be seen that the turbulence intensities in the three directions decreased with increase of the mean wind speed. The higher values of turbulence intensity for mean wind speed between 4 m/s and 6 m/s might be due to the instability of the wind flow. At higher wind speeds such an effect weakened, resulting in that the turbulence intensity values became smaller and their variations with mean wind speed were relatively stable.

3.3 Gust factor and peak factor

The gust factor is a ratio between a peak wind speed within a given data segment and the mean

wind speed of the same segment. The gust factors in the longitudinal, lateral and vertical directions can be calculated by the following equation

$$G_u(t_g) = 1 + \frac{\max(\overline{u(t_g)})}{U}, \quad G_v(t_g) = \frac{\max(\overline{v(t_g)})}{U}, \quad G_w(t_g) = \frac{\max(\overline{w(t_g)})}{U} \quad (2)$$

where t_g is gust duration (in this paper, $t_g=3s$); $\max(\overline{u(t_g)})$, $\max(\overline{v(t_g)})$ and $\max(\overline{w(t_g)})$ are the largest mean wind speed over duration of t_g in longitudinal (u), lateral (v) and vertical (w) directions

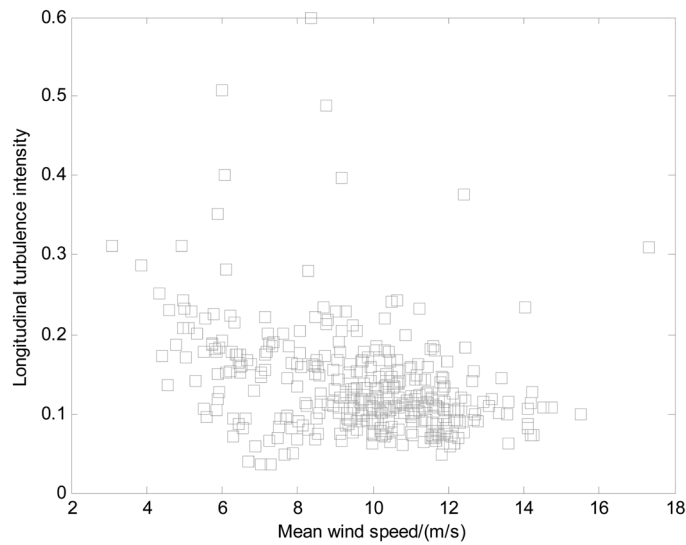


Fig. 5(a) Variation of the longitudinal turbulence intensity with the mean wind speed

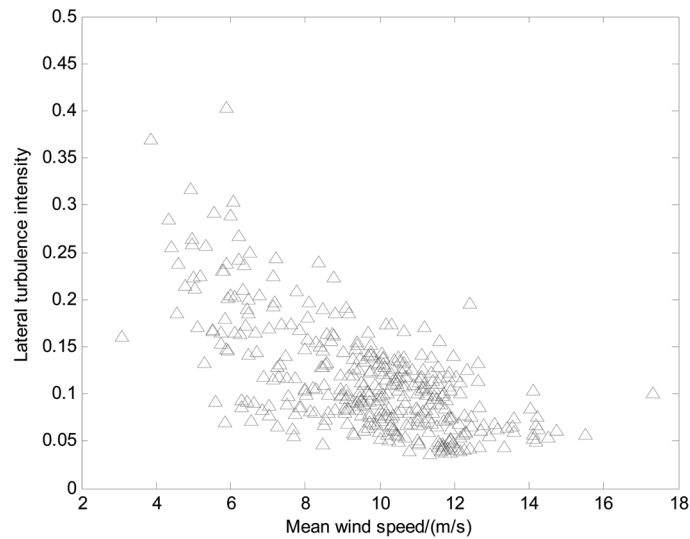


Fig. 5(b) Variation of the lateral turbulence intensity with the mean wind speed

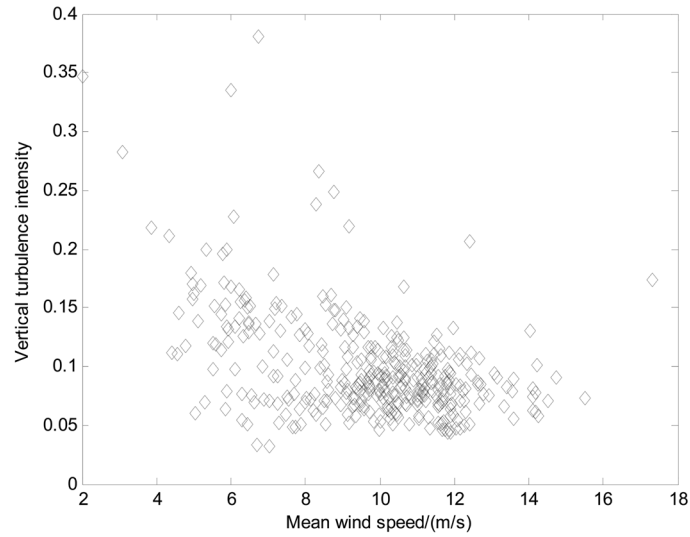


Fig. 5(c) Variation of the vertical turbulence intensity with the mean wind speed

within 10 minutes, respectively.

Fig. 6 shows the polar plots of the longitudinal, lateral and vertical gust factors, respectively, of 10 min duration during the typhoons. It can be seen that the values of the gust factors, in particular those of the longitudinal component, are not very sensitive to the incident wind direction. The mean values of the longitudinal, lateral and vertical gust factors were 1.23, 0.28 and 0.22, respectively. The ratio of the gust factors among the three components is $G_u : G_v : G_w = 1 : 0.23 : 0.18$. Fig. 7 shows the variations of the gust factors measured by the ultrasonic anemometer with the mean wind speed. It is found that the gust factors in the three directions decreased with increase of the mean wind speed and tended to approach constants as the wind speed became large.

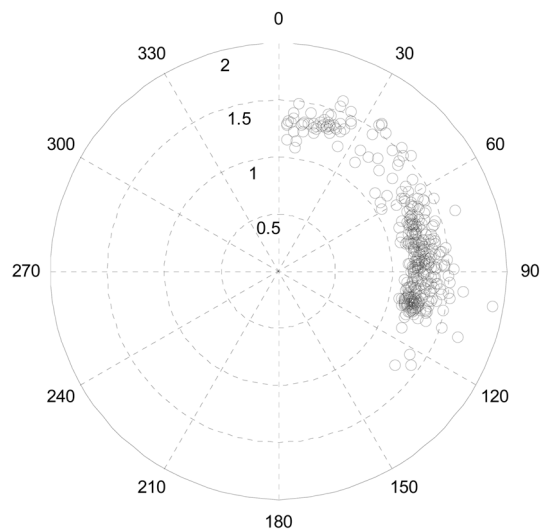


Fig. 6(a) Variation of the longitudinal gust factor with the mean wind direction

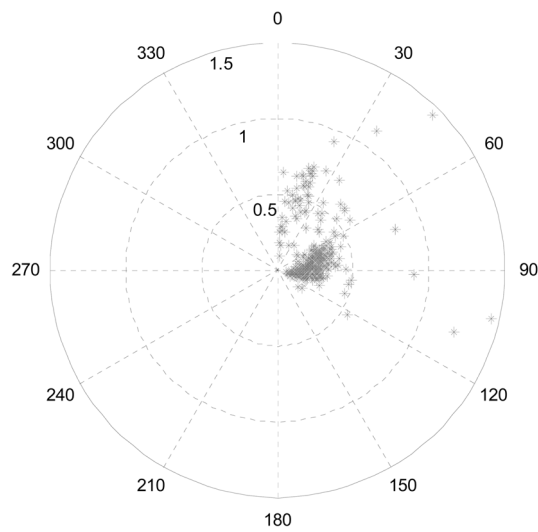


Fig. 6(b) Variation of the lateral gust factor with the mean wind direction

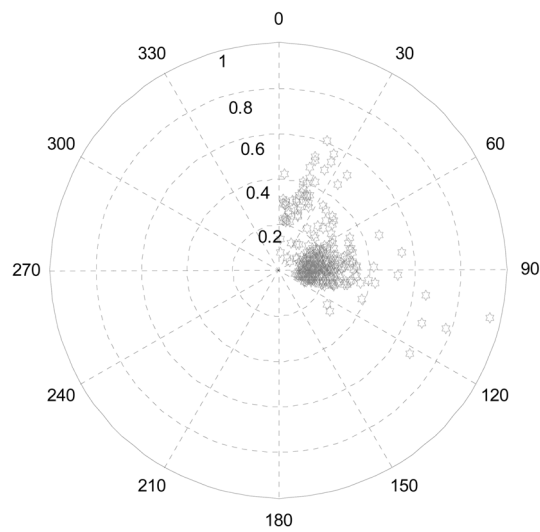


Fig. 6(c) Variation of the vertical gust factor with the mean wind direction

For the relationships among the longitudinal gust factor, longitudinal turbulence intensity and time duration, Ishizaki (1983) and Choi (1983) separately proposed empirical equations. These formulas were combined into one equation by Cao *et al.* (2009) as

$$G_u = 1 + k_1 \times I_u^{k_2} (T/t_g) \quad (3)$$

where T is the averaging time of the mean wind speed. Ishizaki (1983) suggested $k_1 = 0.5$, $k_2 = 1.0$ and Choi (1983) proposed $k_1 = 0.62$, $k_2 = 1.27$.

In this study, the relationship of the gust factor with the turbulence intensity in the longitudinal

direction shown in Fig. 8 was fitted by an equation: $Gu = 1 + 0.33 \times I_u^{0.89} \ln(T/t_g)$. Comparing the fitted curve with the empirical expression described in Eq. (3), it was found that the Ishizaki's linear formula overestimates the gust factor values and Choi's equation generally provide smaller predictions of the gust factor values for low turbulence intensity ($I_u < 0.2$). This implies that the relationship between the gust factor and turbulence intensity actually depends on several factors such as measurement heights and terrain conditions etc.

Peak factor of wind speed is a ratio of the maximum wind speed fluctuation to the standard deviation of the wind speed fluctuation, that is $g_u = \max(u(t))/\sigma_u$. Fig. 9 shows the dependence

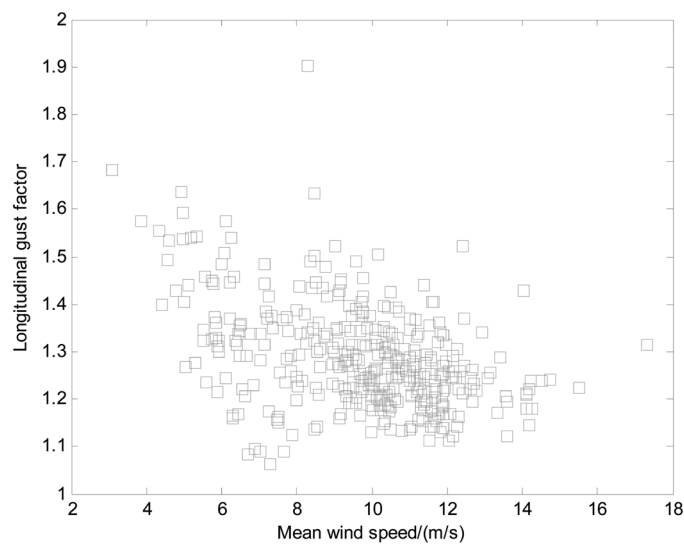


Fig. 7(a) Variation of the longitudinal gust factor with the mean wind speed

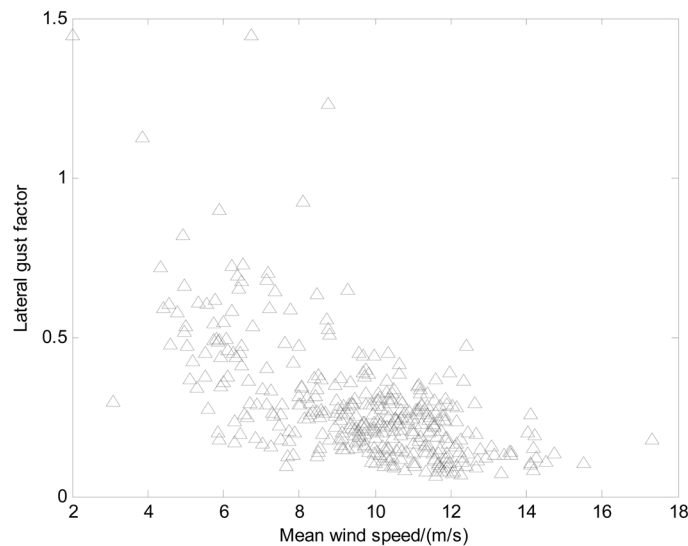


Fig. 7(b) Variation of the lateral gust factor with the mean wind speed

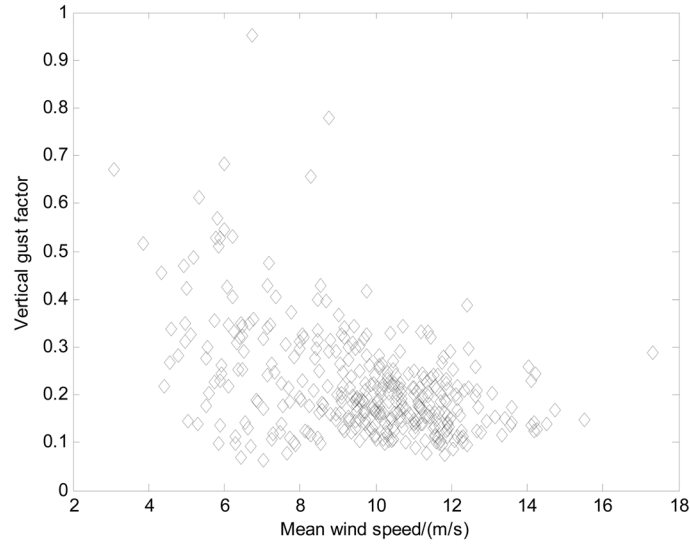


Fig. 7(c) Variation of the vertical gust factor with the mean wind speed

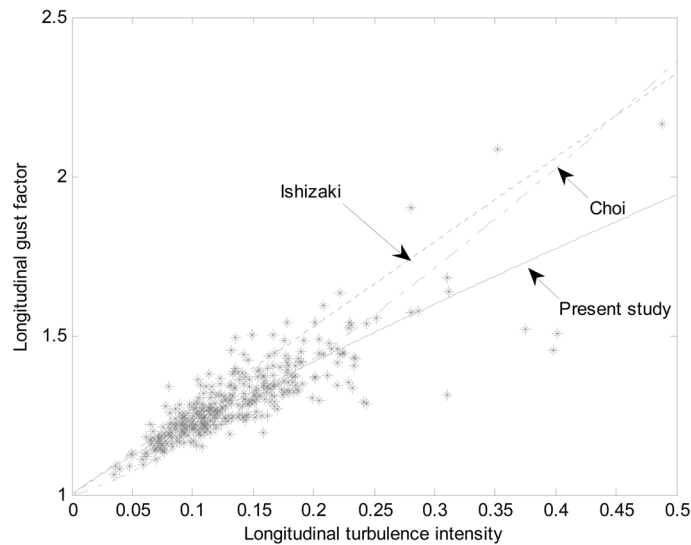


Fig. 8 Variation of the gust factor with the longitudinal turbulence intensity

of the peak factor on the mean wind speed. The mean value of the peak factor derived from the ultrasonic anemometer during the two typhoons is 3.02, which is almost unchanged with the wind speed and wind direction.

3.4 Turbulence integral length scale

Turbulence integral length scale is another important parameter for describing turbulence characteristics of wind flows. It is well known that the parameter varies greatly in atmospheric

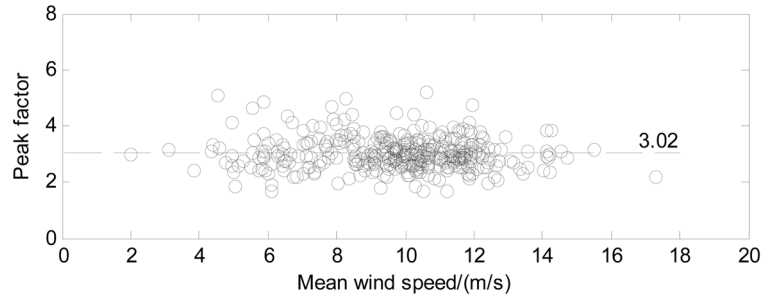


Fig. 9 Variation of the peak factor with the mean wind speed

boundary layer and the determination method also significantly influences the values of the parameter (Li *et al.* 1998). In this study, the turbulence integral length scale is calculated from

$$L_i^x = \frac{U}{\sigma_i} \int_0^\infty R(\tau) d\tau, (i = u, v, w) \tag{4}$$

where $R(\tau)$ is the auto correlation function of fluctuating wind speed in each direction. Fig. 10 shows variations of the turbulence integral length scale values in the three orthogonal directions with the longitudinal mean wind speed. It can be seen from the figure that the variations of the turbulence scales in the three directions were quite large during the typhoons. The average values of the turbulence integral length scale in the longitudinal, lateral and vertical direction during the typhoons were found to be 181 m, 135 and 99 m, respectively. In AIJ-RLB-1996, the longitudinal turbulence integral length scale can be estimated by the empirical expression: $L_u^x = 100(z/30)^{0.5}$.

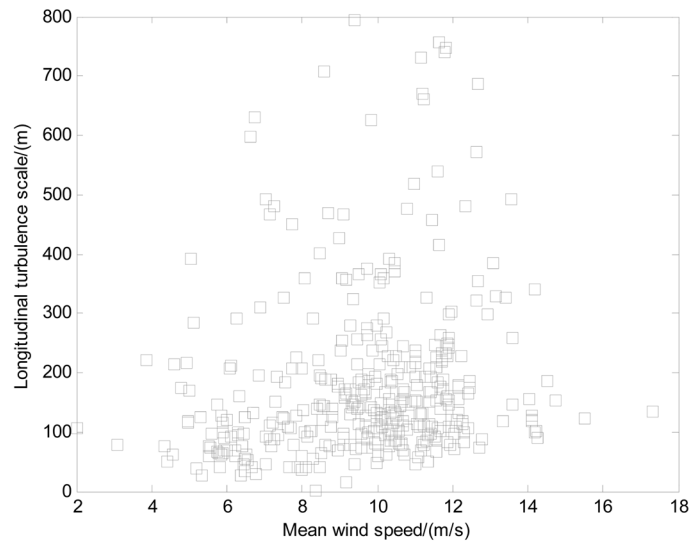


Fig. 10(a) Variation of the longitudinal turbulence integral length scale with the mean wind speed

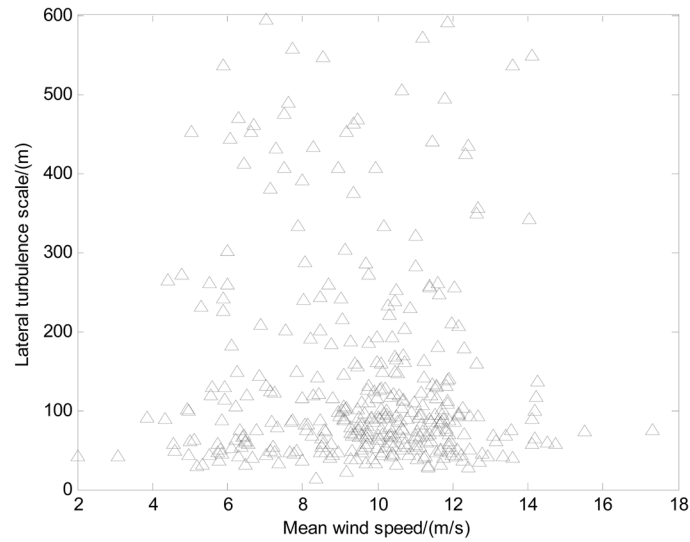


Fig. 10(b) Variation of the lateral turbulence integral length scale with the mean wind speed

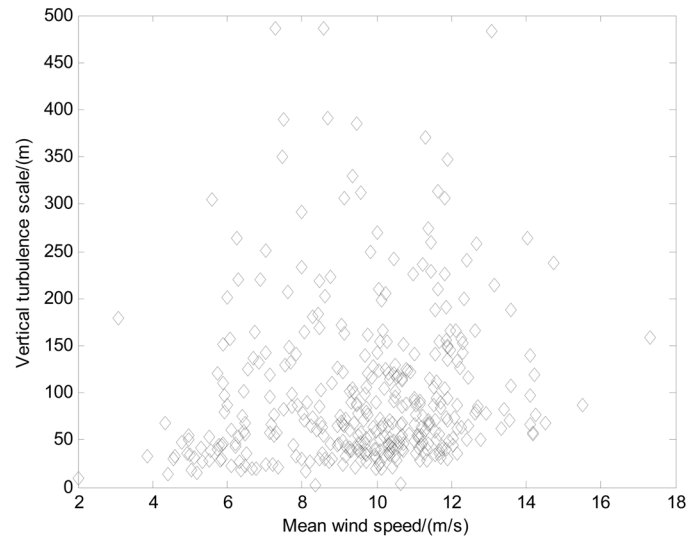


Fig. 10(c) Variation of the vertical turbulence integral length scale with the mean wind speed

The value of the longitudinal turbulence scale at the anemometer location calculated from this equation is 342.8 m which is much larger than the measured mean value, implying that the prediction formula recommended by AIJ may overestimate the longitudinal turbulence integral length scale.

Fig. 11 shows the variation of the longitudinal turbulence integral length scale with the standard deviation of fluctuating wind speed component, which demonstrates that there is no clear relationship between the two parameters during the typhoons.

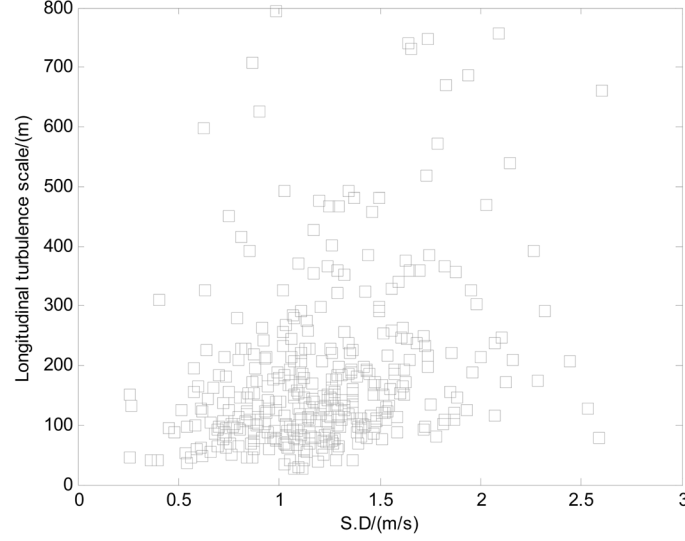


Fig. 11 Variation of the longitudinal turbulence integral length scale with the standard deviation of wind speed

3.5 Power spectral density of wind speed

The energy distribution of fluctuating wind speed can be expressed in the form of power spectral density (PSD). There have been several empirical expressions of power spectral density available for describing wind energy distribution over frequency in atmospheric boundary layer (von Karman 1948, Panofsky and McCormick 1959, Davenport 1961, Kaimal *et al.* 1972)

$$\frac{nS_u(n)}{\sigma_u^2} = \frac{4L_u^x n/U}{[1 + 70.7(L_u^x n/U)^2]^{5/6}} \quad \text{von Karman(Longitudinal)}$$

$$\frac{nS_i(n)}{\sigma_i^2} = \frac{4L_i^x n/U[1 + 755.2(L_i^x n/U)^2]}{[1 + 283.2(L_i^x n/U)^2]^{11/6}}, \quad i = v, w; \quad \text{von Karman(Lateral and Vertical)}$$

$$\frac{nS_u(n)}{kU(10)^2} = \frac{4x^2}{[1 + x^2]^{4/3}}, \quad x = \frac{1200n}{U(10)} \quad \text{Davenport(Longitudinal)} \quad (5)$$

$$\frac{nS_v(n)}{U^{*2}} = \frac{15f}{(1 + 9.5f)^{5/3}}, \quad f = \frac{nz}{U} \quad \text{Kaimal(Lateral)}$$

$$\frac{nS_w(n)}{U^{*2}} = \frac{6f}{(1 + 4f)^2}, \quad f = \frac{nz}{U} \quad \text{Panofsky(Vertical)}$$

where n is frequency; z is the height of the anemometer location; $U(10)$ is the mean wind speed at

10 m height from the ground; κ is assumed to be 0.026; U^* is friction velocity.

In order to discuss the dependency of the PSD functions on the approaching wind directions and identify the potential effects of local topography, an investigation was carried out by analyzing the data measured from the incident wind directions in the sectors with 60-90 and 90-120 degrees. In this study, the power spectral density functions were computed based on the wind data records from the ultrasonic anemometer atop the building with a threshold value of mean wind speed 10 m/s. Fig. 12

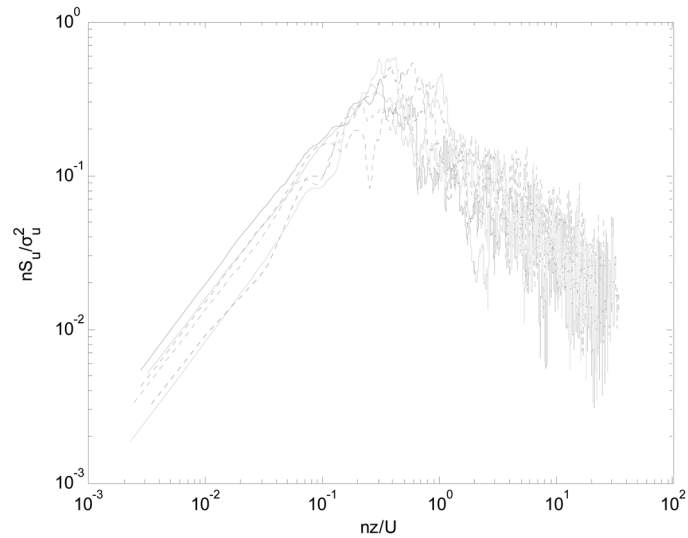


Fig. 12(a) Power spectral density of longitudinal wind speed during the typhoons (The PSD curves for sectors 60-90 degrees and 90-120 degrees are denoted by dot lines and solid lines, respectively.)

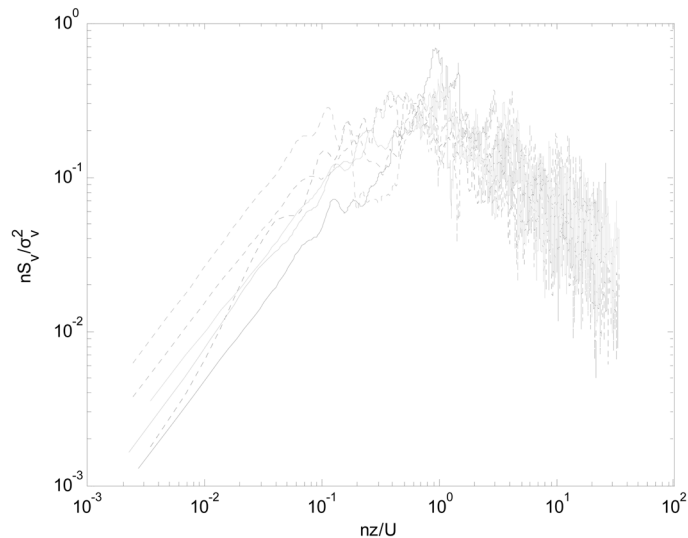


Fig. 12(b) Power spectral density of lateral wind speed during the typhoon (The PSD curves for sectors 60-90 degrees and 90-120 degrees are denoted by dot lines and solid lines, respectively.)

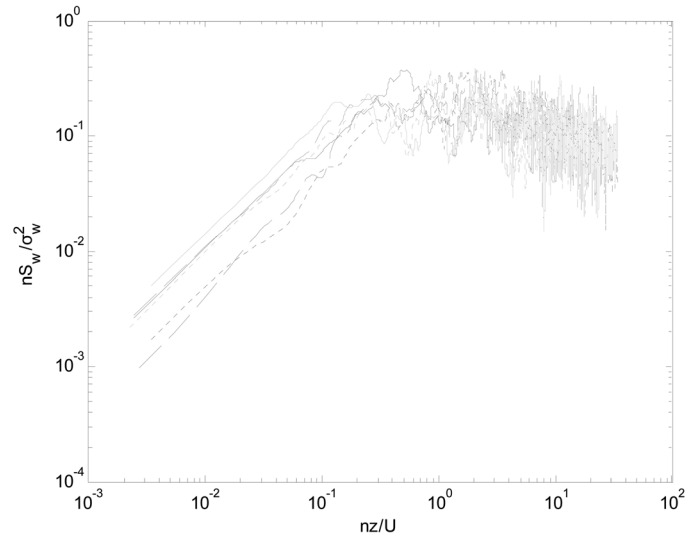


Fig. 12(c) Power spectral density of vertical wind speed during the typhoons (The PSD curves for sectors 60-90 degrees and 90-120 degrees are denoted by dot lines and solid lines, respectively.)

shows some PSD functions of the three wind speed components (longitudinal, lateral and vertical directions) for both the sectors 60-90 degrees (dot lines) and the sector 90-120 degrees (solid lines). The spectra are normalized with respect to $\sigma_i^2 (i = u, v, w)$ and are plotted as a function of $f = nz/U$. It is observed the PSD functions of fluctuating wind speed in the three orthogonal directions in the low-frequency range are essentially similar and do not show clear dependency on the approaching wind directions. A similar trend can also be found in the high-frequency range. It appears that the power spectral density functions of fluctuating wind speed at such a high level over an urban region

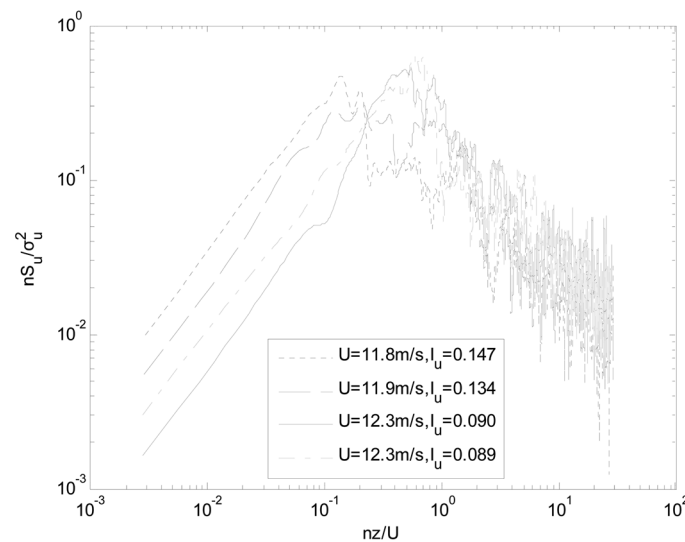


Fig. 13(a) Power spectral density of longitudinal wind speed for various values of I_u

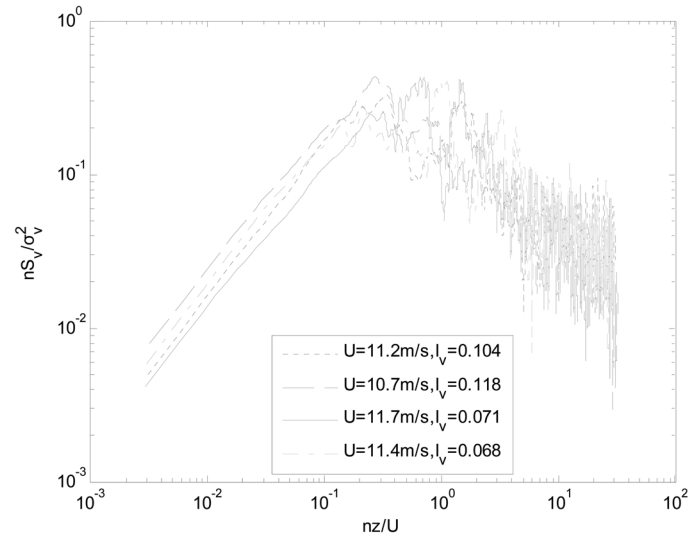


Fig. 13(b) Power spectral density of lateral wind speed for various values of I_v

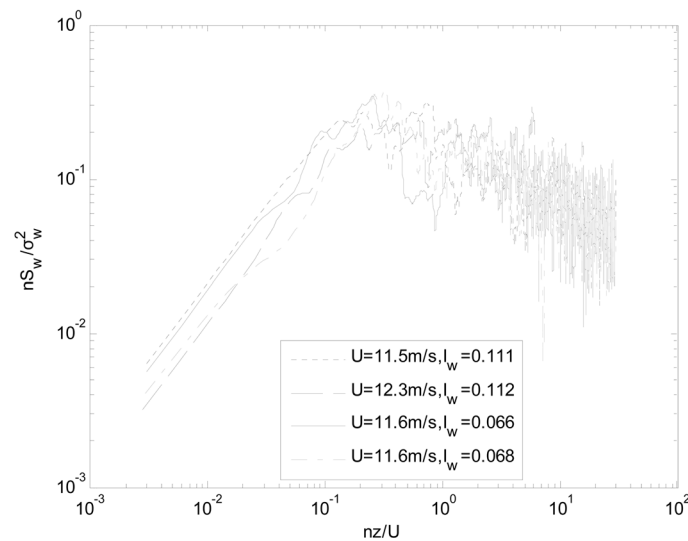


Fig. 13(c) Power spectral density of vertical wind speed for various values of I_w

show limited dependency on the terrain conditions around the tall building. Fig. 13 shows several field measured spectra in the three directions for a variety of turbulence intensities I_i ($i = u, v, w$). The spectra clearly indicate that for increasing values of the turbulence intensities, the longitudinal and lateral wind speed spectra's peaks simultaneously shift to lower values of f . However, less influence is visible in Fig. 13(c) for the spectra of vertical wind speed component. Fig. 14 shows the variations of the longitudinal wind speed spectra with nLu/U . The measured wind speed spectra's peaks all shift to higher values of nLu/U with increase of the turbulence integral length scale during the typhoons.

It is interesting to compare the empirical spectral models with the field measured spectra. The

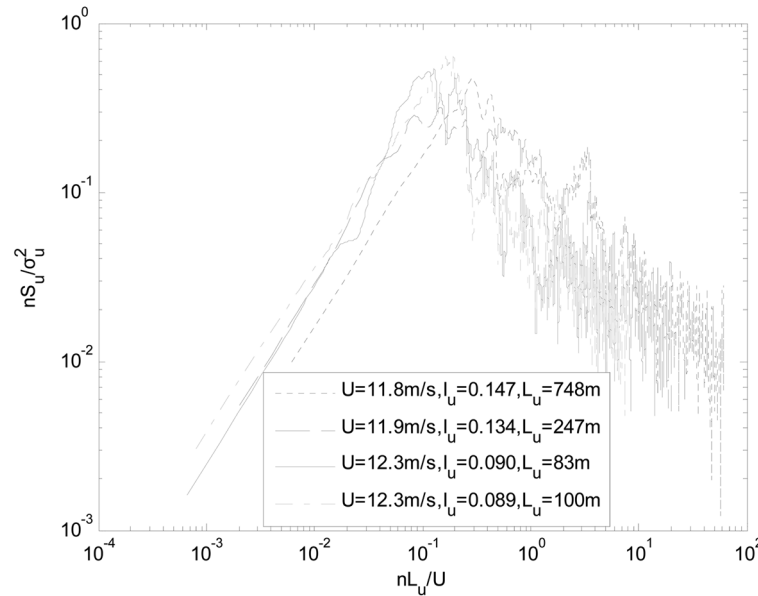


Fig. 14 Power spectral density of longitudinal wind speed

normalized auto-power spectral density functions of fluctuating wind speed in the three orthogonal directions obtained based on the measured wind data during the typhoons are plotted in Figs. 15(a), (b) and (c). For comparison purposes, the empirical spectral models described in Eq.(6) are also presented in the figures, in which the parameters (wind speed and friction velocity etc.) were determined based on the measured results. It can be seen from the figures that the Davenport spectral model decreases too rapidly in the low-frequency range compared with the field measured spectra in the longitudinal direction. There are also some differences between the Panofsky spectral

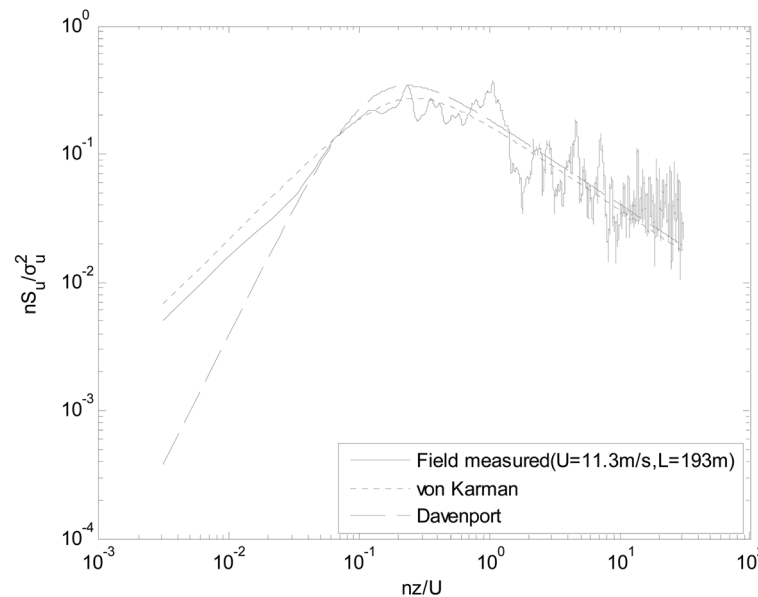


Fig. 15(a) Power spectral density of longitudinal wind speed

Fig. 15(a) Power

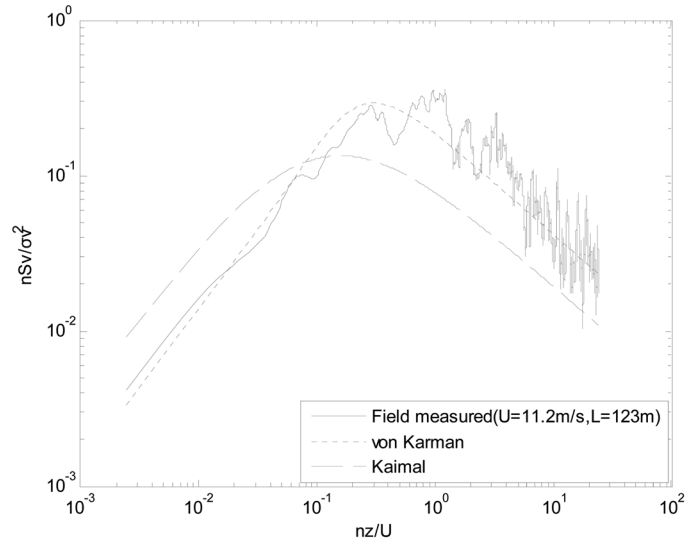


Fig. 15(b) Power spectral density of lateral wind speed

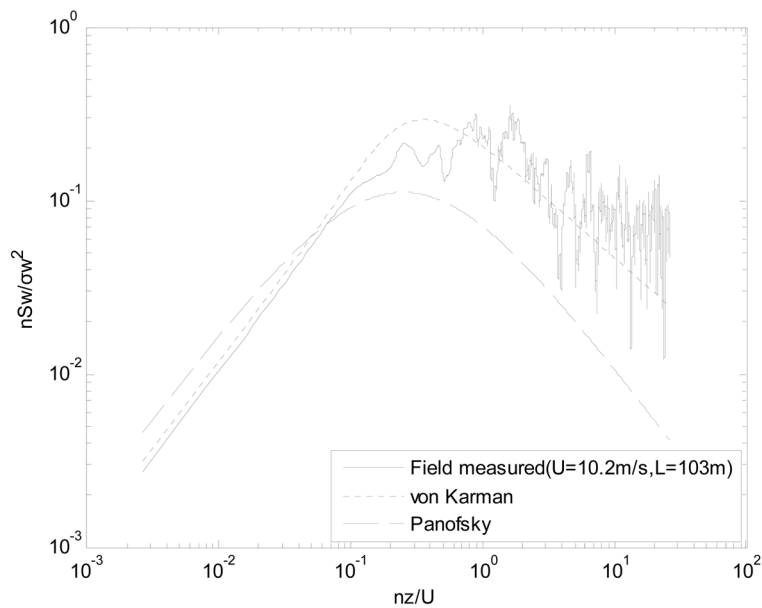


Fig. 15(c) Power spectral density of vertical wind speed

model and those from the field measurements at high frequencies. Obvious differences between the Kaimal spectral model and the measured spectra are observed in the whole frequency range. On the other hand, the von Karman spectra are found to fit the measured power spectral densities in the longitudinal, lateral and vertical directions well, as shown in these figures. This suggests that the von Karman-type spectra are able to describe the energy distribution fairly well for the three components of wind speed above a typical city central district.

4. Dynamic characteristics of CITIC plaza

4.1 Natural frequencies

Natural frequencies of vibration were estimated from the power spectra obtained from a Fast Fourier Transform of the acceleration responses measured from CITIC Plaza during the typhoons, as shown in Fig. 16 and Table 2. This is so-called Peak-Picking method. The spectral analysis results show that the acceleration responses of the super-tall building are primarily in the two fundamental sway modes of vibration, but higher modes are also clearly present. The measured natural frequencies during the two typhoons are very similar, implying that the measured results are reliable. Furthermore, the natural frequencies were also estimated by the Random Decrement Technique (RDT) method as shown in Table 2. The natural frequencies estimated by the PP method and the RDT method are in good agreement.

Natural frequencies must be accurately estimated at the design stage to allow for wind tunnel prediction of equivalent static wind loads and acceleration responses for structural design. Several empirical formulas which are a function of building height are available for evaluating the natural frequencies of tall buildings. Ellis (1980) suggested a formula for the fundamental frequency $f_1 = 46/h$ (where h is building height, m) for all structural types of buildings. Tamura *et al.* (2000) also proposed an empirical expression $f_1 = 67/h$ for reinforced concrete buildings (RC-buildings), based on field measurements taken in Japan. Obviously, the natural frequencies for RC-buildings by Tamura *et al.* give higher values than Ellis' formula. In this study, as the building height of CITIC Plaza is about 391 m from the ground, the calculated values of the fundamental frequency from the two equations by Ellis and Tamura are 0.118 Hz and 0.171 Hz, respectively, while the measured values during the typhoons are in the range of 0.170-0.172 Hz. The measured natural frequency of the RC-building is in very good agreement with that determined by the empirical formula

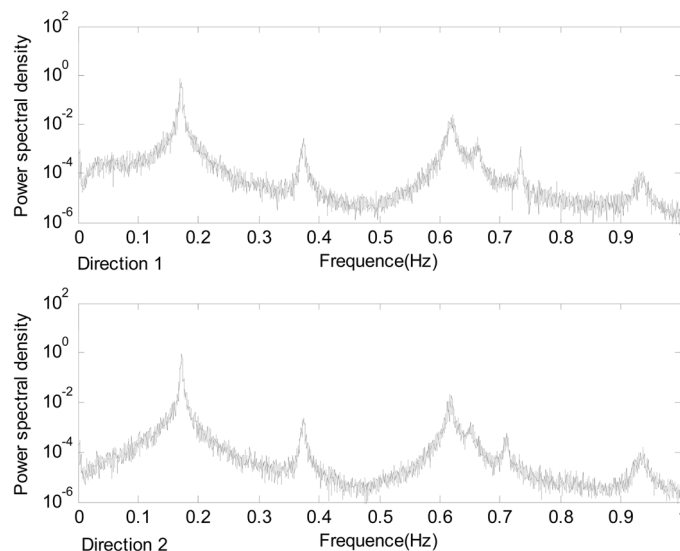


Fig. 16(a) Power spectral density of acceleration responses during Typhoon Damrey

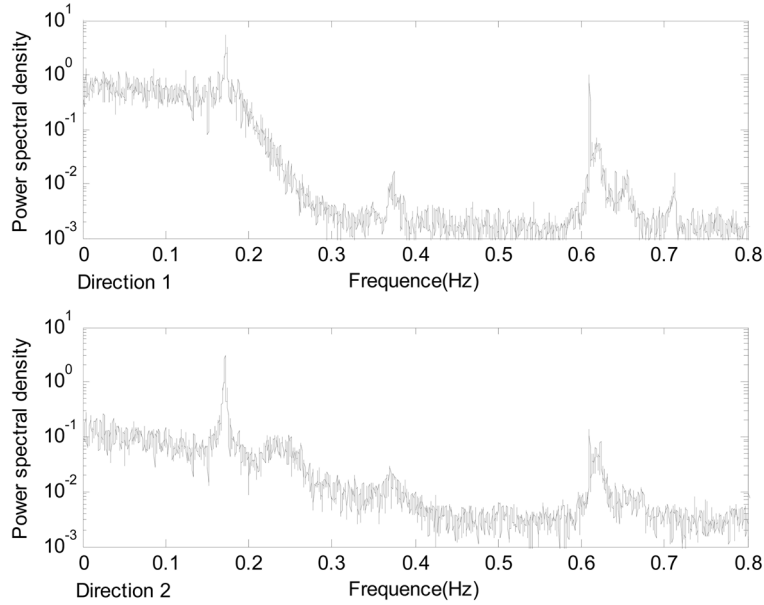


Fig. 16(b) Power spectral density of acceleration responses during Typhoon Pabuk

Table 2 Natural frequencies of CITIC Plaza

| | | Direction X | | Direction Y | |
|-----|----------|-------------|-------------|-------------|-------------|
| | | Mode 1 (Hz) | Mode 2 (Hz) | Mode 1 (Hz) | Mode 2 (Hz) |
| PP | “Damrey” | 0.170 | 0.620 | 0.173 | 0.617 |
| | “Pabuk” | 0.172 | 0.618 | 0.171 | 0.618 |
| RDT | “Damrey” | 0.170 | 0.618 | 0.172 | 0.617 |
| | “Pabuk” | 0.172 | 0.611 | 0.170 | 0.618 |

recommended by Tamura *et al.*, implying that the formula is applicable to dynamic analysis of RC tall buildings at preliminary design stages.

4.2 Correlation of numerical results and field measurements

A three-dimensional Finite Element (FE) model of CITIC Plaza was established based on the structural design drawings, as shown in Fig. 17. 3-D shell elements, which has both bending and membrane capabilities, were employed to model floors. The columns and beams were modeled with 3-D beam elements. The connection between the structure and its foundation was treated to be fixed. The first five natural frequencies and mode shapes determined by the FE model, including two modes for translational motions in each horizontal direction and one mode for rotational motion about the vertical axis, are shown in Table 3 and Fig. 18, respectively. For comparison purposes, the measured natural frequencies of the building and the differences between the numerical results and the full-scale measurements are listed in Table 3. It can be seen from Table 3 that there are about 15.2–27.5% differences between the calculated and measured natural frequencies for the first two sway modes in both directions. The differences between the calculated and measured natural



Fig. 17 FE model

Table 3 Measured and calculated natural frequencies

| Modes | Measured* [Hz] | Calculated [Hz] | Difference* [%] |
|-----------------------|----------------|-----------------|-----------------|
| Mode 1 in direction 1 | 0.171 | 0.145 | 15.2 |
| Mode 1 in direction 2 | 0.172 | 0.143 | 16.8 |
| Rotational | 0.374 | 0.213 | 43.0 |
| Mode 2 in direction 1 | 0.617 | 0.447 | 27.5 |
| Mode 2 in direction 2 | 0.618 | 0.452 | 26.8 |

*Measured = Overall average values of the natural frequencies measured during the two typhoons

*Difference = (Measured-calculated)/Measured.

frequencies are attributable to several reasons, including that the effective mass values of the buildings are less than those assumed at the design stage, or/and the effective stiffness values of the buildings are higher than those determined at the design stage due to the contribution of nonstructural components. As a result, the measured natural frequencies for the two fundamental sway modes of CITIC Plaza are larger than those calculated.

4.3 Damping characteristics

To determine the damping ratios of this tall building during the typhoons, the Random Decrement Technique (RDT) assuming stationary white noise inputs was employed. The reliability and accuracy of the RDT method for structural modal parameter identification based on ambient vibrations measurement has been evaluated by Jeary (1986), Li *et al.* (2003, 2004a), Tamura and Suganuma (2003), Kijewski and Kareem (2002). As commented by Li *et al.* (2003) among others, the random decrement technique represents a quick and practical method for establishing the nonlinear damping characteristics. As discussed above, the wind-induced response of the building is primarily in the two fundamental sway modes of vibration, but higher modes are also present. In order to obtain the damping ratio of each mode, the measured signals of the stationary response data

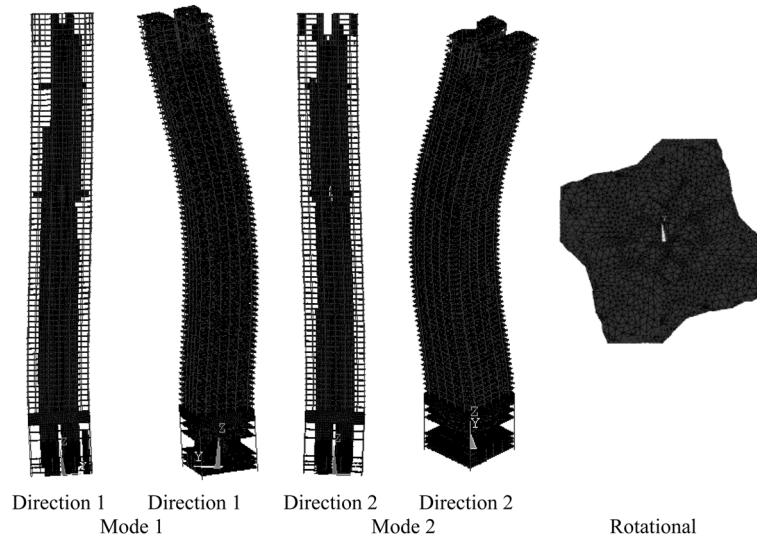


Fig. 18 Mode shapes by FEM

were band-pass filtered before processing the random decrement technique to remove the components not concerned. The information on the damping ratios against vibration amplitude for the first two sway mode in each direction are shown in Fig. 19. It can be observed from the figure that the damping curves demonstrated two distinct regimes. The damping ratios in low amplitude region are relatively scatter and their variations with amplitude become stable when the vibration amplitude becomes higher. This phenomenon may be explained using Fig. 20 which shows the acceleration spectra corresponding to three levels of vibration amplitudes. In low amplitudes, the proportions of noise signals involved in the records relative to the structural resonant responses may be larger than those in higher amplitudes. In such cases, the noise signals will infiltrates the RDT algorithm, and the resonant contributions cannot be fully isolated, which may lead to inaccurate damping estimates. However, as resonant amplitude increases, its proportion in an overall record of measured acceleration data becomes more significant. This enables isolation of the resonant responses in the estimation of damping ratios. Furthermore, it is also found from Fig. 19 that the damping curves in direction 1 demonstrate amplitude-dependent characteristics and increased with increasing vibration amplitude during the typhoons. However, the damping results in direction 2 remain almost unchanged regardless of the variation of the vibration amplitude. This may be attributed to relatively lower levels of vibration amplitudes in direction 2. From the measurements of damping, it is found that the overall fundamental modal damping ratios of the super-tall building mainly varied in range of 0.5%-2.0%. It appears that damping value of 1.0% of critical is reasonable for wind-resistant design of the super-tall building for serviceability consideration.

5. Acceleration responses and comparison with wind tunnel test results

5.1 Acceleration response analysis

Fig. 21 shows the relationships between the reduced wind speed (U_r) and the RMS values of the

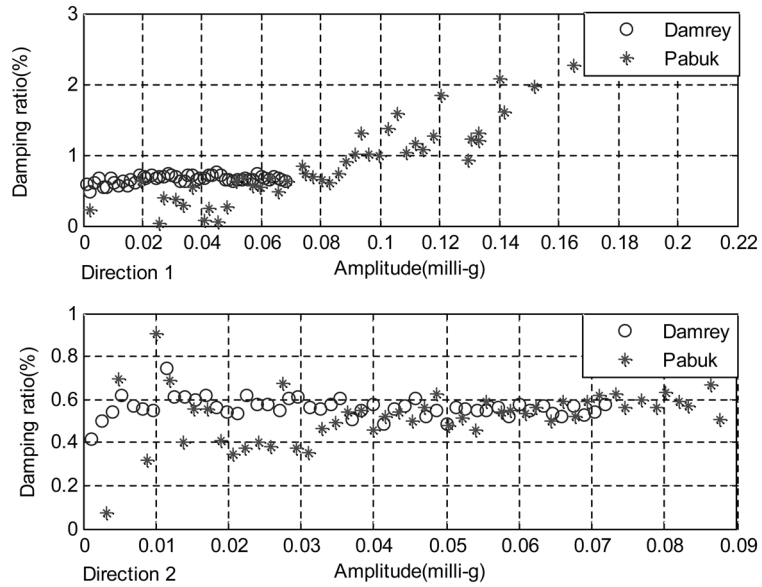


Fig. 19(a) Variation of damping ratio of the first mode with amplitude

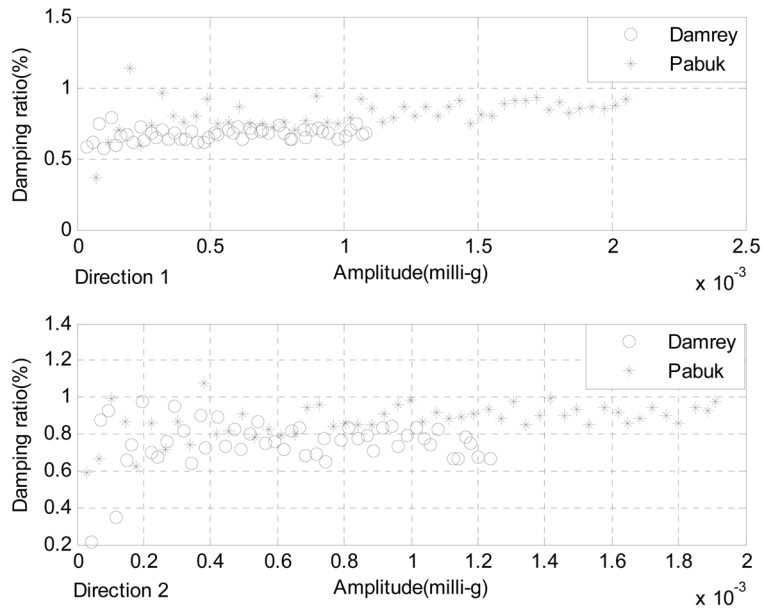


Fig. 19(b) Variation of damping ratio of the second mode with amplitude

10-minute averaged acceleration responses in directions 1 and 2 for southeasterly winds with mean wind direction of 103° during the typhoons. For the data presented in Fig. 21, the regression curves of the acceleration response for each direction are expressed by

$$\sigma_a = c_1(U_r)^{c_2} \quad (\text{milli-g}) \tag{7}$$

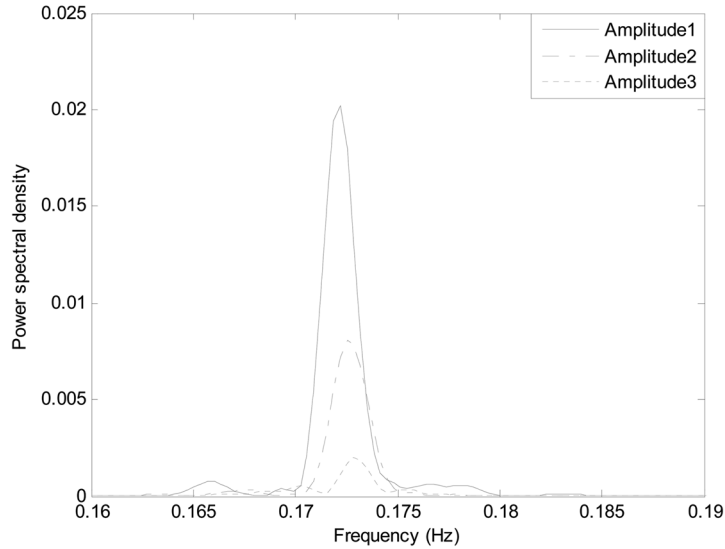


Fig. 20 PSDs for three amplitude regimes (Amplitude 1 > Amplitude 2 > Amplitude 3)

where σ_a is the RMS acceleration response; U_r is the reduced wind speed ($U_r = U_H / (n_0 B)$); is the fundamental natural frequency of the building; B represent the building width; c_1 and c_2 are the curve fitting parameters; U_H is the 10-min mean wind speed at the top of the building, which can be obtained from the mean wind speed measured at the anemometer at height of 352.5 m based on the power law with exponent of 0.22 as follows

$$U_H = \frac{U}{(352.5/H)^{0.22}} \quad (8)$$

where H is the reference height (the building roof height).

It can be seen from Fig. 21(a) that the increase in the dynamic acceleration response in direction 1 was associated with the increases in the reduced wind speed. Fig. 21(b) also shows the same tendency for direction 2. The RMS acceleration responses along the two directions are proportional to the reduced wind speed raised to a power of 2.55 and 2.99, respectively.

5.2 Serviceability evaluation

For super-tall buildings, such as the CITIC Plaza, keeping the wind-induced motions during strong wind storms within acceptable limits may be a more challenge task than ensuring that they have sufficient structural strength. It has been widely accepted that building acceleration is the most common index for evaluating structural serviceability performance under wind actions. A number of proposals and regulations dealing with serviceability criteria for tall buildings subjected to wind-induced vibrations have been suggested. Some codes, for example, the National Building Code of Canada (1991) suggests acceptable levels of accelerations as a serviceability requirement, which recommends that a tentative maximum acceleration limitation of 1 to 3 percent of gravity (10-30 *milli-g*) once every 10 years as a guideline for comfort of occupants and that the lower value might be considered applied

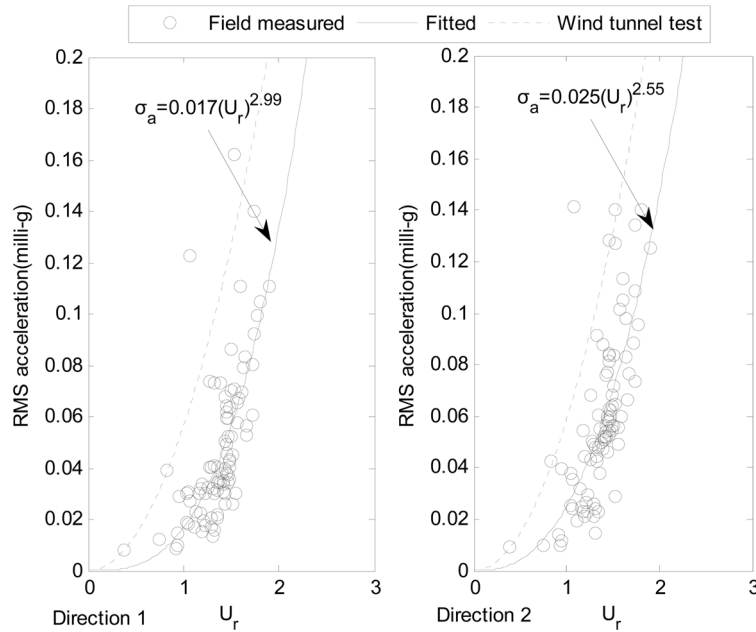


Fig. 21 Relationship between the RMS acceleration responses and the reduced wind speed

to apartment buildings, while the higher value for office buildings. ISO 6897 (1984) suggests a RMS acceleration criterion for a 5-year return period for building structures which include the structural natural frequency dependence. The suggested criterion can be summarized as follows

$$a(rms) = 2.65 \times n_0^{-0.41} \text{ (milli-g)} \tag{9}$$

where $a(rms)$ is RMS acceleration response and n_0 is the fundamental natural frequency (Hz) of a building.

In order to assess the serviceability of the tall building properly, the relationship among the resultant acceleration responses and the mean wind speed as well as the occupancy comfort criteria for different return periods is discussed herein. The RMS values of the resultant wind-induced acceleration response can be determined by taking the square root of the sum of the squares (SRSS) of the acceleration responses in direction 1 and direction 2. Fig. 22 shows the forecasting resultant acceleration responses from the two components of the building motions, which were obtained based on the field measurements. For comparison purposes, the serviceability criteria for return periods of 5 years (ISO 6897) and 10 years (NBCA) are also plotted in the figure. The NBCA criterion of RMS acceleration was determined from the maximum acceleration criterion divided by a peak factor of 3.5. The wind speeds with the return periods (5 and 10 years) marked in the figure were obtained from the wind climate information of Guangzhou (2006). It can be seen from the figure that the super-tall building would appear to satisfactorily meet the occupancy comfort criterion of ISO6897 and the Canadian criterion.

5.3 Comparison with the wind tunnel results

It is very useful to compare the field measured results with those from wind tunnel tests for the

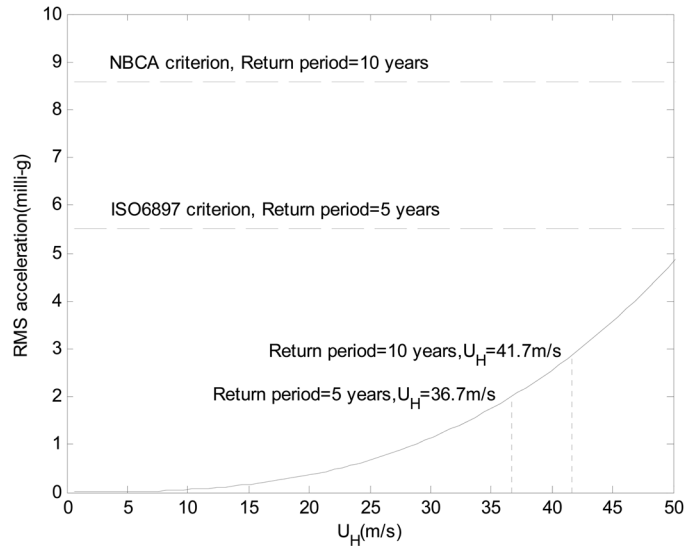


Fig. 22 Comparison of the resultant acceleration responses predicted based on the field measurements and the serviceability criteria of ISO6897 and NBCA

purposes of evaluating the accuracy of the model test results and the adequacy of the modeling techniques used in wind tunnel tests. In fact, such comparisons are quite rare for super-tall buildings under typhoon conditions.

At the design stage of the tall building, detailed wind tunnel studies for evaluating its wind-induced responses was carried out in the boundary layer wind tunnel laboratory at Monash University in 1993 through aeroelastic model tests (Cheung *et al.* 1993). The predicted wind-induced building responses, including the design wind loads and building accelerations, were then used in the structural design. By sorting the RMS acceleration responses under the mean wind direction around 103 degree from the southeast, the comparison of the measured accelerations atop the tall building with those predicted from the wind tunnel test are plotted in Fig. 21 for direction 1 and 2. It can be seen from the figure that the predicted results are consistent with the real structural responses, but generally larger than the measured data and appear to represent envelopes of the measured RMS responses. In other words, the model test provided conservative predictions of the acceleration responses at the design stage. This is acceptable in engineering practices.

6. Conclusions

This paper presents selected results measured from CITIC Plaza based on the installed monitoring system during two typhoons. Detailed analysis of the measured data and numerical results was carried out and some conclusions are summarized as follows:

(1) The average values of the turbulence intensities in the longitudinal, lateral and vertical directions during the two typhoons were 0.14, 0.12 and 0.10, respectively. The mean values of the longitudinal, lateral and vertical gust factors were 1.23, 0.28 and 0.22, respectively. The values of the turbulence intensity and gust factor in the three directions decreased with increase of the mean

wind speed during the typhoons. The values of the peak factor were almost unchanged with the mean wind speed and wind direction. The ratios of the turbulence intensities among the three components obtained during the two typhoons were $I_u : I_v : I_w = 1 : 0.86 : 0.71$. The measured average longitudinal turbulence intensity value was in good agreement with that determined by AIJ-1996.

(2) Variations of the turbulence integral length scales in the three directions were observed to be quite large during the typhoons. The prediction formula recommended by AIJ was found to overestimate the mean value of the longitudinal turbulence integral length scale during the typhoons. The spectral peaks of the longitudinal and lateral wind speed components shifted to lower values of with increasing values of the turbulence intensities in these directions. The von Karman spectra were found to be able to describe the energy distribution quite well for wind speeds in the longitudinal, lateral and vertical directions above a typical city central district.

(3) The natural frequencies measured from CITIC Plaza during the two typhoons were very similar, illustrating that the dependency of the natural frequencies with the vibration amplitudes of the tall building was negligible. The estimates of the natural frequencies obtained by the PP method and the RDT method were in good agreement. A three-dimensional Finite Element model was constructed for the numerical dynamic analysis of the super-tall building. The calculated natural frequencies of the first several modes were compared with those determined from the field measurements. The differences between the calculated and measured natural frequencies for the first two sway modes in both directions were about 15.2–27.5%, while the numerical analysis provided underestimations of the natural frequencies.

(4) Damping ratios in low amplitude region were quite scatter and became stable when the vibration amplitude becomes relative larger. It was also found that the measured damping ratios demonstrated nonlinear energy dissipation characteristic and increased with increasing amplitude. The measurement results implied that damping ratios of 1.0% of critical appear reasonable for wind-resistant design of super-tall buildings for serviceability consideration.

(5) Wind-induced acceleration responses of the tall building during the two typhoons were found to be increased with increase of the reduced wind speed. The RMS values of the acceleration responses along the two directions were proportional to the reduced wind speed raised to a power of 2.55 and 2.99, respectively. From the forecasting resultant acceleration responses which were obtained based on the field measurements, the super-tall building would appear to satisfactorily meet the occupancy comfort criterion of ISO6897 and the Canadian criterion for different return periods. A comparison of the acceleration responses of the CITIC Plaza with the wind tunnel test predictions has been made. It was observed that the predicted results from the model test were consistent with the real structural responses, but generally larger than the measured data and appeared to represent envelopes of the measured RMS responses.

Acknowledgments

The work described in this paper was fully supported by grants from the Research Grants Council of Hong Kong Special Administrative Region, China (Project No: CityU 116906 and CityU 117709) and a research grant from the Research Committee of City University of Hong Kong (Project No. 7002615).

References

- AIJ-RLB-1996. (1996), "Recommendations for loads on buildings", Architecture Institute of Japan.
- Campbell, S., Kwok, K.C.S., Hitchcock, P.A., Tse, K.T. and Leung, H.Y. (2007), "Field measurements of natural periods of vibration and structural damping of wind-excited tall residential buildings." *Wind Struct.*, **10**(5), 401-420.
- Cao, S.Y., Tamura, Y., Kikuchi, N., Saito, M., Nakayama, N. and Matsuzaki, Y. (2009), "Wind characteristics of a strong typhoon", *J. Wind. Eng. Ind. Aerod.*, **97**(1), 11-21.
- Cheung, J.C.K., Palmer, T.R. and Melbourne, W.H. (1993), Aeroelastic wind tunnel model tests on Tian Ho Commercial Development, Guangzhou, PRC. MEL Consultant Report 14/93, Monash University.
- Choi, E.C.C. (1983), Wind loading in Hong Kong: commentary on the Code of Practice on Wind Effects Hong Kong-1983, Hong Kong Institution of Engineers, Hong Kong.
- Climate and Agricultural Meteorology Institute of Guangdong. (2006), Report on meteorological analysis and calculation at Guangzhou West Tower, Guangdong Meteorological Bureau, Guangzhou, P.R. China.
- Davenport, A.G. (1961), "The spectrum of horizontal gustiness near the ground in high winds", *Q. J. Roy. Meteor. Soc.*, **87**(372), 194-211.
- Ellis, B.R. (1980), "An assessment of the accuracy of predicting the fundamental natural frequencies of buildings and the implications concerning the dynamic analysis of structures", *Proceedings of the Inst. Struct. Engineers*, **69**(3), 763-776.
- GB50009-2001. (2002), Load code for the design of building structures, China Architecture & Building Press, Beijing.
- Ishizaki, H. (1983), "Wind profiles, turbulence intensities and gust factors for design in typhoon-prone regions", *J. Wind. Eng. Ind. Aerod.*, **13**(1-3), 55-66.
- ISO 6897 (1984), Guidelines for the evaluation of the response of occupants of fixed structures, especially buildings and off-shore structures, to low-frequency horizontal motion.
- Jeary, A.P. (1986), "Damping in tall buildings, a mechanism and a predictor", *Earthq. Eng. Struct. D.*, **14**(5), 773-750.
- Kaimal, J.C., Wyngaard, J.C., Izumi, Y. and Cote, O.R. (1972), "Spectral characteristics of surface-layer turbulence", *Q. J. Roy. Meteor. Soc.*, **98**, 563-589.
- Kijewski, T. and Kareem, A. (2002), "On the reliability of a class of system identification techniques: insights from bootstrap theory", *Struct. Saf.*, **24**(2-4), 261-280.
- Kijewski -Correa, T.L. (2003), Full-scale measurements and system identification: a time-frequency perspective, PhD Thesis, The University of Notre Dame.
- Li, Q.S., Fang, J.Q., Jeary, A.P. and Wong, C.K. (1998), "Full scale measurement of wind effects on tall buildings", *J. Wind. Eng. Ind. Aerod.*, **74-76**, 741-750.
- Li, Q.S., Yang, K., Wong, C.K. and Jeary, A.P. (2003), "The effect of amplitude-dependent damping on wind-induced vibrations of a super tall building", *J. Wind. Eng. Ind. Aerod.*, **91**(9), 1175-1198.
- Li, Q.S., Xiao, Y.Q., Wong, C.K. and Jeary, A.P. (2004a), "Full-scale measurements of typhoon effects on a super tall building", *Eng. Struct.*, **26**(2), 233-244.
- Li, Q.S. and Wu, J.R. (2004b), "Correlation of dynamic characteristic of a super tall building from full-scale measurements and numerical analysis with various finite element models", *Earthq. Eng. Struct. D.*, **33**(14), 1311-1336.
- Li, Q.S., Xiao, Y.Q. and Wong, C.K. (2005), "Full-scale monitoring of typhoon effects on super tall buildings", *J. Fluid. Struct.*, **20**(5), 697-717.
- Li, Q.S., Fu, J.Y., Xiao, Y.Q., Li, Z.N., Ni, Z.H., Xie, Z.N. and Gu, M. (2006), "Wind tunnel and full-scale study of wind effects on China's tallest building", *Eng. Struct.*, **28**(12), 1745-1758.
- Littler J.D. and Ellis B.R. (1992), "Full scale measurements to determine the response of Hume Point to wind loading", *J. Wind. Eng. Ind. Aerod.*, **42**(1-3), 1085-1096.
- National Building Code of Canada, (1991), National Research Council. Ottawa, Canada.
- Ohkuma, T., Marukawa, H., Niihori, Y. and Kato, N. (1991), "Full-scale measurement of wind pressures and response accelerations of a high-rise building", *J. Wind. Eng. Ind. Aerod.*, **38**(2-3), 185-186.
- Panofsky, H.A. and McCormik, R.A. (1959), The spectrum of vertical velocity near the surface, Collection of

- Mineral industries, Pennsylvania University, University Park.
- Pirnia, J.D., Kijewski-Correa, T., Abdelrazaq, A., Chung, J.Y. and Kareem, A. (2007), "Full-scale validation of wind-induced response of tall buildings: investigation of amplitude-dependent properties", *Proceedings of the Struct. Congress ASCE*, Long Beach, CA, May.
- Solari, G. and Piccardo, G. (2001), "Probabilistic 3-D turbulence modeling for gust buffeting of structures", *Probabilist. Eng. Mech.*, **16**(1), 73-86.
- Tamura, Y. and Saganuma, S. (1996), "Evaluation of amplitude-dependent damping and natural frequency of buildings during strong winds", *J. Wind. Eng. Ind. Aerod.*, **59**(2-3), 115-130.
- Tamura, Y., Suda, K. and Sasaki, A. (2000), "Damping in buildings for wind resistant design", *Proceedings of the Int. Symp. on Wind and Structures for the 21st Century*, Cheju, Korea.
- Tamura, Y., Yoshida, A. and Zhang, L. (2005), "Damping in buildings and estimation techniques", *Proceedings of the 6th Asia-Pacific Conf. on Wind Engineering*, Seoul, Korea.
- Von Karman, T. (1948), "Progress in the statistical theory of turbulence", *P. Natl. Acad. Sci. USA*, **34**(11), 530-539.
- Panofsky, H. A. and McCormik, R. A. (1959), *The spectrum of vertical velocity near the surface*, *Collection of Mineral industries*, Pennsylvania University, University Park.
- Pirnia, J.D., Kijewski-Correa, T., Abdelrazaq, A., Chung, J.Y. and Kareem, A. (2007), "Full-scale validation of wind-induced response of tall buildings: investigation of amplitude-dependent properties", *Proc. Struct. Congress ASCE*, Long Beach, CA, 16-19, May.
- Solari, G., and Piccardo, G. (2001), "Probabilistic 3-D turbulence modeling for gust buffeting of structures", *Probabilist. Eng. Mech.*, **16**, 73-86.
- Tamura, Y., and Saganuma, S. (1996), "Evaluation of amplitude-dependent damping and natural frequency of buildings during strong winds", *J. Wind. Eng. Ind. Aerod.*, **59**, 115-130.
- Tamura, Y., Suda, K. and Sasaki, A. (2000), "Damping in buildings for wind resistant design", *Proceedings of the Int. Symp. on Wind and Structures for the 21st Century*, Cheju, Korea, 115-130.
- Tamura, Y., Yoshida, A. and Zhang, L. (2005), "Damping in buildings and estimation techniques", *Proceedings of the 6th Asia-Pacific Conf. on Wind Engineering*, Seoul, Korea, 193-214.
- von Karman, T. (1948), "Progress in the statistical theory of turbulence", *Proceedings of the National Academy of Sciences*, **34**, 530-539.